

F-box and Leucine-rich Repeat Protein 5 (FBXL5) Is Required for Maintenance of Cellular and Systemic Iron Homeostasis*[§]

Received for publication, October 7, 2012, and in revised form, November 6, 2012. Published, JBC Papers in Press, November 7, 2012, DOI 10.1074/jbc.M112.426171

Julio C. Ruiz^{‡1}, Scott D. Walker[‡], Sheila A. Anderson[§], Richard S. Eisenstein[§], and Richard K. Bruick^{‡2}

From the [‡]Department of Biochemistry, University of Texas Southwestern Medical Center, Dallas, Texas 75390-9038 and the [§]Department of Nutritional Sciences, University of Wisconsin, Madison, Wisconsin 53706

Background: FBXL5 is an iron-responsive E3 ubiquitin ligase.

Results: FBXL5-null mice die during embryogenesis, whereas *Fbxl5* heterozygotes perform better than wild type littermates when fed a low iron diet due to enhanced iron absorption.

Conclusion: FBXL5 plays an essential role in the *in vivo* maintenance of cellular and systemic iron homeostasis.

Significance: FBXL5 is an essential physiological iron sensor.

Maintenance of cellular iron homeostasis requires post-transcriptional regulation of iron metabolism genes by iron regulatory protein 2 (IRP2). The hemerythrin-like domain of F-box and leucine-rich repeat protein 5 (FBXL5), an E3 ubiquitin ligase subunit, senses iron and oxygen availability and facilitates IRP2 degradation in iron replete cells. Disruption of the ubiquitously expressed murine *Fbxl5* gene results in a failure to sense increased cellular iron availability, accompanied by constitutive IRP2 accumulation and misexpression of IRP2 target genes. FBXL5-null mice die during embryogenesis, although viability is restored by simultaneous deletion of the *IRP2*, but not *IRP1*, gene. Mice containing a single functional *Fbxl5* allele behave like their wild type littermates when fed an iron-sufficient diet. However, unlike wild type mice that manifest decreased hematocrit and hemoglobin levels when fed a low-iron diet, *Fbxl5* heterozygotes maintain normal hematologic values due to increased iron absorption. The responsiveness of IRP2 to low iron is specifically enhanced in the duodena of the heterozygotes and is accompanied by increased expression of the divalent metal transporter-1. These results confirm the role of FBXL5 in the *in vivo* maintenance of cellular and systemic iron homeostasis and reveal a privileged role for the intestine in their regulation by virtue of its unique FBXL5 iron sensitivity.

Iron is widely employed throughout biology. Failure to maintain bioavailable iron concentrations within appropriate levels may result in deleterious consequences ranging from anemia to

iron overload disease (1, 2). IRPs³ regulate the post-transcriptional expression of several iron metabolism genes upon binding iron responsive elements (IREs) within the 5' or 3' untranslated regions (UTRs) of their mRNAs in iron-depleted cells (3, 4). For example, synthesis of the iron storage protein ferritin heavy chain 1 is reduced upon binding of IRPs to its 5' IRE (5). Conversely, iron uptake is promoted by stabilization of the mRNAs encoding the iron import factors transferrin receptor 1 (TfR1) and DMT-1 upon IRP binding to IREs within their 3' UTRs (4, 6). As iron bioavailability increases, IRPs lose their RNA binding capacity either through conformational changes resulting from the enhanced FeS cluster assembly within IRP1 (3) or enhanced proteasomal degradation of IRP2 (7).

Selective degradation of IRP2 is preceded by its iron-dependent polyubiquitination via a Skp1/Cul1/Rbx1 (SCF) E3 ubiquitin ligase complex containing FBXL5 (8, 9). FBXL5 contains an N-terminal hemerythrin-like domain characterized by a helical bundle held together by a di-iron center (8–11). When iron and oxygen are abundant, this domain resides in a compact conformation that masks a degron within the hemerythrin-like domain itself, promoting FBXL5 accumulation and subsequent IRP2 degradation (11, 12). When low levels of bioavailable iron limit assembly of the di-iron center, the hemerythrin-like degron becomes accessible and FBXL5 is degraded by the proteasome (11–13). These properties of the FBXL5 hemerythrin-like domain suggest that it is a key sensor of bioavailable ferrous iron within cells (14). The importance of FBXL5 to the maintenance of cellular iron homeostasis was initially confirmed through siRNA-mediated knockdown of FBXL5 expression, which resulted in inappropriate stabilization of IRP2 in iron-replete cells (8). Such cells aberrantly repress ferritin expression while promoting continued iron uptake through stabilization of the TfR1 mRNA (8, 9, 15), exacerbating the metabolic stress of excessive iron.

To investigate the *in vivo* role for FBXL5 in the maintenance of iron homeostasis, we generated mice in which the *Fbxl5* gene locus has been disrupted. FBXL5-null mice die during embryo-

* This work was supported, in whole or in part, by National Institutes of Health Grants HL102481 (to R. K. B.), DK66600 (to R. S. E.), and GM084266 (to P. A. L.), a Career Award in the Biomedical Sciences from the Burroughs Wellcome Fund (to R. K. B.), and Robert A. Welch Foundation Grant I-1568 (to R. K. B.).

⌘ Author's Choice—Final version full access.

§ This article contains supplemental "Materials and Methods," Tables S1–S4, and Figs. S1–S3.

¹ HHMI Scholar and supported by a Sara and Frank McKnight Graduate Student Fellowship.

² Michael L. Rosenberg Scholar in Medical Research. To whom correspondence should be addressed: 5323 Harry Hines Blvd., K3.112, Dallas, TX 75390-9038. Tel.: 214-648-6477; E-mail: richard.bruick@utsouthwestern.edu.

³ The abbreviations used are: IRP, iron regulatory proteins; FbxL5, F-box and leucine-rich repeat protein 5; IRE, iron responsive element; TfR1, transferrin receptor 1; GT, gene trapping; DMT-1, divalent metal transporter-1; SCF, Skp1/Cul1/Rbx1.

genesis due to unregulated IRP2 accumulation. *Fbxl5* heterozygotes, although viable, exhibit an unexpected phenotype. Unlike their wild type littermates, these mice maintain their hematocrit and hemoglobin levels when challenged with a low iron diet. Here we show that although *Fbxl5* heterozygosity has little apparent effect on the iron-responsive behavior of most tissues, iron absorption through the duodenum is substantially altered. These results suggest that the FBXL5-dependent iron sensitivity of the cells within the intestine is set differently from other cells in the body and, as a consequence, FBXL5 plays a previously unrecognized role in systemic iron homeostasis.

EXPERIMENTAL PROCEDURES

Animals—Murine 129 Sv/Ev embryonic stem cells heterozygous for the gene-trapped *Fbxl5* allele (clone OST386421) were obtained from Texas A&M Institute for Genomic Medicine and injected into C57Bl/6J blastocysts at the University of Texas Southwestern (UTSW) Transgenic Technology Center. The resulting chimeric mice were crossed to C57Bl/6J mice (Jackson Laboratories) to produce heterozygous animals. Backcrossing *Fbxl5* heterozygous mice of mixed background to wild type 129 Sv/Ev mice resulted in the generation of syngeneic *Fbxl5*^{+/*GT*} mice that were 99.99% of 129 Sv/Ev genetic background as determined by speed congenics (Taconic). *Fbxl5* wild type and *Fbxl5* heterozygous mice were weaned onto a *ad libitum* iron-sufficient (50 ppm) or low iron (5 ppm) diet (Harlan-Teklad) for 3 weeks. For the ⁵⁹Fe feeding experiments, mice fed a low iron diet for 3 weeks were then fasted for 24 h and gavaged with an olive-tipped needle containing 200 μl of PBS supplemented with 2.5 μCi of ⁵⁹FeCl₃ (PerkinElmer Life Sciences) and 0.5 M ascorbic acid. At the indicated time points, animals were exsanguinated and ⁵⁹Fe accumulation in tissues was measured in a Packard Cobra Gamma Counter. Blood samples were collected from the tail vein or via cardiac puncture following intraperitoneal administration of anesthetic rodent mixture (ketamine/xylazine/acepromazine). Complete Blood Count analysis was performed by the UTSW Diagnostic Lab. Serum iron concentration, iron saturation, and total iron binding capacity were measured by Idexx Laboratories, Cornell University. The *Irf1*^{-/-} and *Irf2*^{-/-} (16, 17) mice were generously provided by Matthias Hentze. All animal experiments were performed with the approval of the UTSW Institutional Animal Care and Use Committee.

Isolation, Culture, and Characterization of Mouse Embryonic Cells—Mouse embryonic cells were prepared as described (18). Briefly, E8 embryos were digested with trypsin at 37 °C for 30 min. Cells were cultured on a layer of mitotic inactivated mouse embryonic fibroblast feeder cells in Dulbecco's modified high glucose Eagle's medium (HyClone) supplemented with 20% fetal bovine serum (Atlanta Biological), 1× nonessential amino acids (HyClone), 1× penicillin and streptomycin (HyClone), 2 mM glutamine (HyClone), 55 μM β-mercaptoethanol (Sigma), and 110 mg/liter of pyruvate (HyClone). After 4 weeks, cells were grown without feeder cells and immortalized upon transfection of the SV40 large T antigen (pSV3-Neo, ATCC) with Lipofectamine 2000 (Invitrogen). Stably transfected cells were selected in the presence of 500 μg/ml of G418.

Additional "Materials and Methods"—See supplemental "Materials and Methods" for supporting information.

RESULTS

FBXL5 Is Ubiquitously Expressed—As all mammalian cells have a requirement for iron, yet are susceptible to damage when bioavailable iron accumulates, a *bona fide* cellular iron sensor should be ubiquitously expressed. FBXL5 mRNA levels were quantitated by quantitative PCR across panels of human and murine tissue extracts. As predicted, FBXL5 expression was detected in all samples with the highest relative levels present in the brain, particularly the metal-rich cerebellum (19), eye, and testis (Fig. 1, A and B). These same FBXL5 mRNA-abundant tissues also tend to express relatively high levels of IRP1 and IRP2 mRNAs (Fig. 1, A and B, and Ref. 20). In the mouse, FBXL5 expression is high at embryonic day (E) 7.5 (Fig. 1B), suggesting a role in early embryogenesis, although its expression decreases as the embryo progresses through development (E11 and E15).

Mice Lacking a Functional FBXL5 Gene Die during Embryogenesis—Insertion of a gene-trapping (GT) vector downstream of the second exon of *FBXL5* generated a disrupted allele (*Fbxl5*^{GT}; Fig. 2). Progeny from mice containing one copy of this nonfunctional allele were genotyped at various developmental time points. Although wild type (*Fbxl5*^{+/+}), heterozygous (*Fbxl5*^{+/*GT*}), and homozygous null (*Fbxl5*^{GT/*GT*}) embryos were initially observed in a Mendelian 1:2:1 ratio, no *Fbxl5*^{GT/*GT*} pups were born (Table 1). In the mixed genetic background of our mice, E9.5 *Fbxl5*^{GT/*GT*} embryos exhibited growth retardation as compared with wild type and heterozygous littermates (Fig. 3A). Although developmentally delayed, histopathological analysis revealed that E9.5 *Fbxl5*^{GT/*GT*} embryos had undergone normal placentation (Fig. 3, B and C), gastrulation, and cardiovascular development (Fig. 3D). However, at E10.5 these embryos appeared very distorted and were completely absorbed by day E12.5.

Iron Metabolism Genes are Aberrantly Regulated in FBXL5^{GT/*GT*} Mouse Embryonic Cells—Given the proposed role of FBXL5 in mediating cellular iron homeostasis, we suspected that *Fbxl5*^{GT/*GT*} embryos would fail to properly regulate IRE-containing mRNAs. Due to the early embryonic lethality of the *Fbxl5*^{GT/*GT*} mice, we generated mouse embryonic cell lines from *Fbxl5*^{+/+}, *Fbxl5*^{+/*GT*}, and *Fbxl5*^{GT/*GT*} embryos (Fig. 4A) harvested on day E8. *Fbxl5*^{+/+} and *Fbxl5*^{+/*GT*} cells depleted of bioavailable iron with the metal chelator deferoxamine mesylate (DFO) strongly accumulate IRP2 compared with iron-replete cells incubated with ferric ammonium citrate. However, *Fbxl5*^{GT/*GT*} cells aberrantly accumulate IRP2 under both conditions (Fig. 4C). Total IRP1 protein levels remained constant under all conditions and in all cell types (Fig. 4C). This inappropriately accumulated IRP2 is competent for IRE binding (Fig. 4D) and *Fbxl5*^{GT/*GT*} cells exhibit increased TfR1 expression and decreased ferritin expression under iron replete conditions (Fig. 4, B and C). An increase in iron uptake, coupled with a decrease in iron storage capacity, could result in the overaccumulation of iron accompanied by increased oxidative stress in these FBXL5-null cells.

To ascertain whether embryonic lethality was due to deregulated IRP2 expression, we crossed *Fbxl5*^{+/*GT*} mice with IRP2

FBXL5 Regulates Iron Metabolism in Vivo

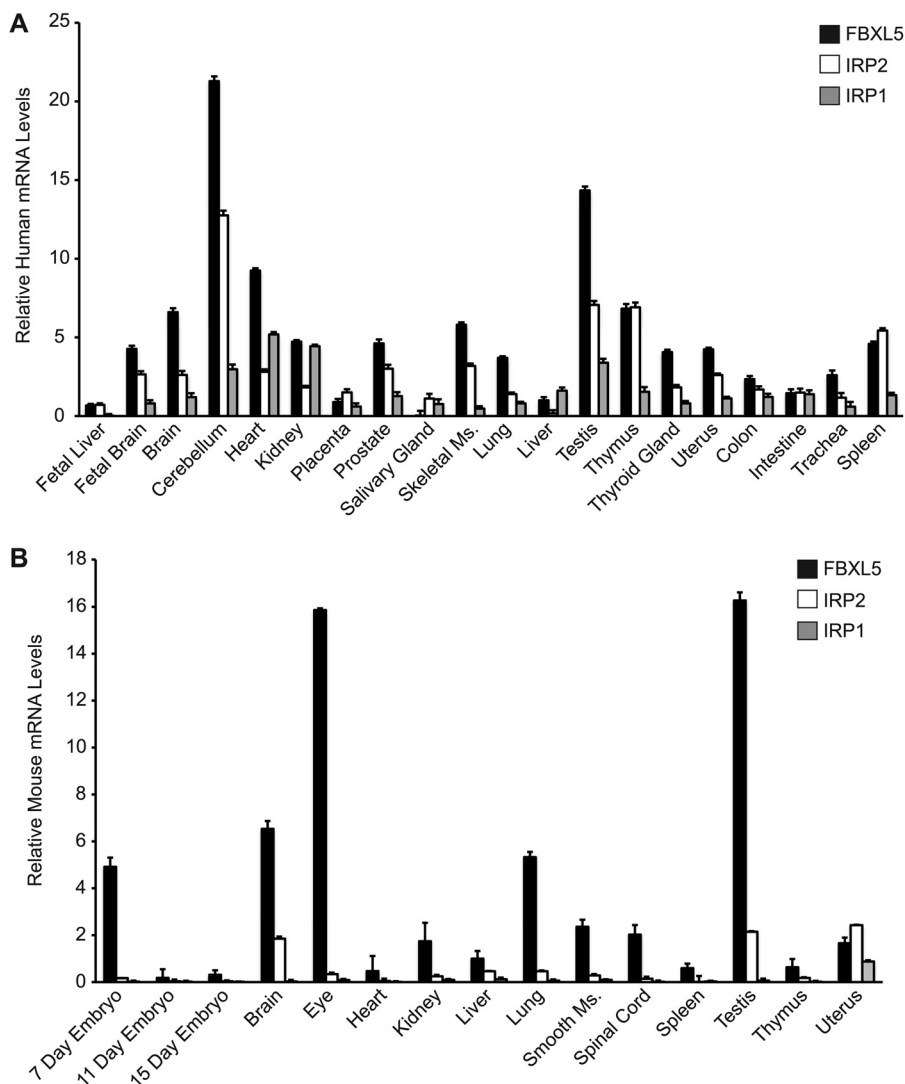


FIGURE 1. **FBXL5 is ubiquitously expressed in humans and mice.** Relative mRNA levels of FBXL5, IRP1, and IRP2 were quantitated by quantitative PCR from human (A) and murine (B) tissue samples. Each column represents the average of three experiments \pm S.D.

knock-out mice (21). Viable *Irp2*^{-/-}; *Fbxl5*^{GT/GT} mice were born from *Irp2*^{+/-}; *Fbxl5*^{+ /GT} intercrosses, although no *Irp2*⁺; *Fbxl5*^{GT/GT} mice were observed (Table 2). Like their littermates, *Irp2*^{-/-}; *Fbxl5*^{GT/GT} mice grow normally and are fertile. This result suggests that the early embryonic mortality of FBXL5-null animals is due to the constitutive accumulation of IRP2 with concomitant dysregulation of its target genes. Interestingly, when *Irp1*^{+/-}; *Fbxl5*^{+ /GT} mice were crossed, no *Irp1*^{-/-}; *Fbxl5*^{GT/GT} pups were observed at birth (Table 3), despite the significant redundancy in IRP1 and IRP2 function (22, 23).

Fbxl5^{+ /GT} Mice Differ from *Fbxl5*^{+/+} Littermates When Fed a Low Iron Diet—To determine whether *Fbxl5*^{+ /GT} mice manifest a non-overt iron-related phenotype(s), we challenged wild type and heterozygous mice with a low iron (5 ppm) diet and compared their results to mice weaned onto an iron-sufficient (50 ppm) diet (23, 24). After 3 weeks ingesting the specified diets, complete blood counts and serum iron levels were determined. Wild type mice fed a low iron diet exhibited an expected 77% decrease in serum iron levels despite a compensatory 149%

increase in the total iron binding capacity of transferrin (Table 4). Consistent with the low dietary iron availability, wild type animals report significant reductions in hematocrit and hemoglobin levels, and a modest reduction in the number of red blood cells (RBC) (Table 4). All measurements taken from *Fbxl5*^{+ /GT} mice fed an iron-sufficient (50 ppm) diet were indistinguishable from control *Fbxl5*^{+/+} mice. Even *Fbxl5*^{+ /GT} mice fed a low iron diet exhibit similar changes in serum iron and total iron binding capacity values to those of their wild type counterparts (Table 4). However, this reduced iron availability does not result in any corresponding reductions in hematocrit, hemoglobin, or erythrocyte levels in the *Fbxl5* heterozygotes (Table 4). To guard against the possibility that this unexpected phenotype was due to the mixed genetic background of these mice, *Fbxl5*^{+ /GT} mice were backcrossed to 129 Sv/Ev mice to generate syngeneic *Fbxl5*^{+ /GT} mice. Just like their mixed background *Fbxl5*^{+ /GT} counterparts, syngeneic *Fbxl5*^{+ /GT} mice still maintained normal hematologic values when fed a low iron diet (Table 5). These data suggest that *Fbxl5*^{+ /GT} mice have altered their systemic iron homeostasis so as to make iron preferen-

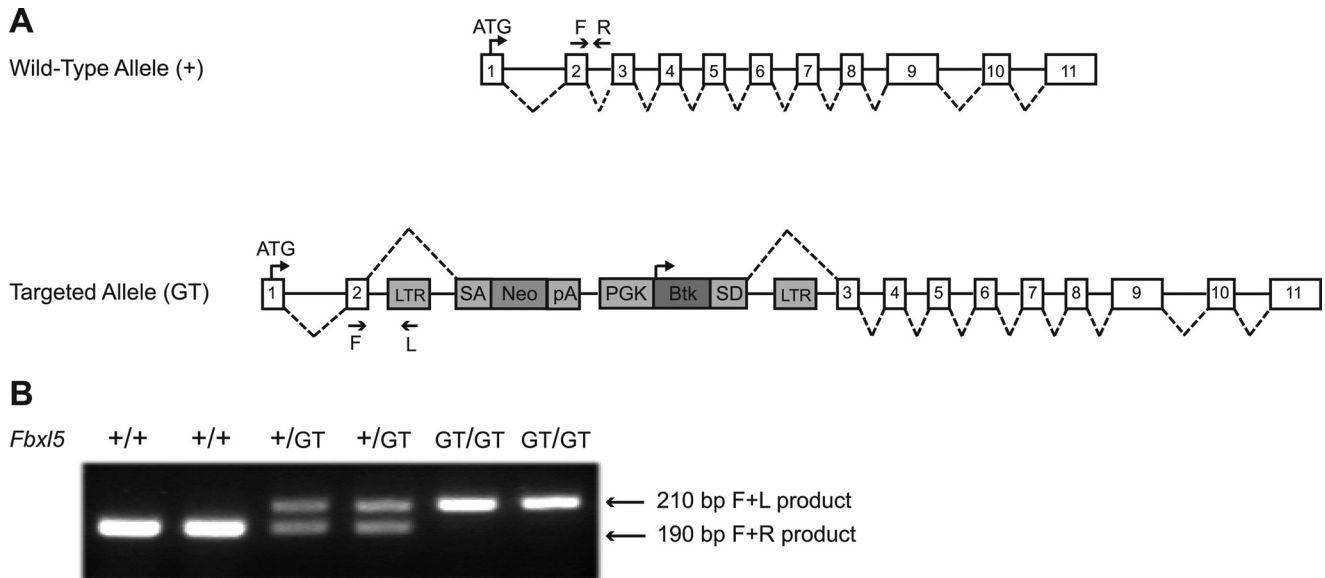


FIGURE 2. **Disruption of the murine *Fbxl5* gene.** *A*, embryonic stem cells containing a gene-trapped (GT) *Fbxl5* allele were used to generate FBXL5-null mice. A trapping vector containing a promoter-less neomycin (*Neo*) resistance cassette flanked by a splicing acceptor (*SA*) site and a polyadenylation signal sequence (*pA*) was inserted 3' of *Fbxl5* exon 2. Utilization of the *SA* site generates a truncated FBXL5 mRNA transcript competent for *Neo* expression. The trapping vector also contains the first exon of the Bruton's tyrosine kinase (*Btk*) gene flanked by the PGK promoter sequence and a splicing donor site (*SD*). The resultant chimeric fusion transcript was used to generate a sequence tag of the trapped gene by 3' RACE. *B*, genotypic analysis by PCR using genomic DNA isolated from wild type mice (*Fbxl5*^{+/+}), heterozygous mice (*Fbxl5*^{+/GT}), or FBXL5-null mice (*Fbxl5*^{GT/GT}).

TABLE 1
Genotypes of embryos from heterozygous matings

Stage	No. of Progeny			Total
	+/+	+/GT	GT/GT	
E9.5	20	44	18	82
E10.5	11	22	9	42
E11.5	12	28	10 ^a	50
E12.5	10	22	0	32
Postnatal	85	155	0	240

^a Partially absorbed embryos.

tially available to the erythroid compartment, irrespective of genetic background.

Iron Absorption and Systemic Distribution Are Altered in *Fbxl5*^{+/GT} Mice Fed a Low Iron Diet—We hypothesized that the requisite iron needed to maintain normal hematocrit and hemoglobin values in *Fbxl5*^{+/GT} mice could be made available either through depletion of iron stores or through increased intestinal absorption. The metal content of the liver, a major site of iron storage (4), was determined by inductively coupled plasma mass spectrometry (supplemental Fig. S1 and Fig. 5). As shown in Fig. 5, total iron content in the liver was reduced in an equivalent amount in all mice fed the low iron diet for 3 weeks, providing no indication that additional iron was mobilized from *Fbxl5*^{+/GT} liver stores.

To determine whether *Fbxl5*^{+/GT} mice are more efficient than wild type mice at absorbing limiting dietary iron, ⁵⁹Fe was directly introduced via gastric gavage into the stomachs of mice that had been fed a low iron diet for 3 weeks and the distribution of ⁵⁹Fe in various tissues was measured over time. After 1 h, almost 80-fold more ⁵⁹Fe was incorporated within the duodena of *Fbxl5*^{+/GT} mice as compared with wild type animals (Fig. 6A). This increased efficiency in intestinal uptake was accompanied by a corresponding 3-fold increase in serum ⁵⁹Fe levels (Fig. 6B). The whole body distribution of ⁵⁹Fe is also markedly

different in the *Fbxl5*^{+/GT} mice, as this newly absorbed iron is made preferentially available to the spleen (Fig. 6C) and the bone marrow (Fig. 6D, femur) for rapid incorporation into red blood cells (Fig. 6E), rather than sites of storage (Fig. 6F, liver).

***Fbxl5* Heterozygosity Specifically Alters the Iron Responsiveness of the Duodenum**—Although *Fbxl5*^{+/GT} mice are indistinguishable from *Fbxl5*^{+/+} mice when fed an iron-sufficient diet, the heterozygous mice take up iron more efficiently when dietary availability is limiting. To determine the underlying cause of this difference, immunoblot analysis was used to examine the expression of iron metabolism genes. In wild type mice fed a low iron diet, intestinal iron absorption is typically promoted in multiple ways. At the cell autonomous level (25, 26), IRP activity is induced within iron-depleted intestinal epithelial cells (supplemental Fig. S2), stabilizing an IRE-containing DMT-1 transcript (supplemental Table S1) and subsequently promoting iron uptake through increased DMT-1 expression (Fig. 7A). At the same time, reduced serum iron levels attenuate hepcidin (HAMP) transcription in the liver (supplemental Table S1) (27). A reduction in circulating hepcidin levels stabilizes the iron export protein ferroportin (Fig. 7A) to facilitate iron absorption through the intestine (27, 28). In the *Fbxl5*^{+/GT} animals, the systemic, ferroportin-dependent, response is identical to *Fbxl5*^{+/+} mice, both at the level of hepcidin expression in the liver (supplemental Table S1) and ferroportin accumulation in the duodenum (Fig. 7A). However, the cell autonomous response to low iron is dramatically altered in the duodena of *Fbxl5*^{+/GT} mice fed a low iron diet. IRP2 protein levels are 7-fold higher than in the corresponding wild type mice (Fig. 7A and supplemental Table S2). The accompanying 2-fold increase in IRP-binding activity (Fig. 7C) mimics the 2-fold additional increase in the IRE-containing DMT-1 mRNA (but not the IRE-independent DMT-1 mRNA isoform; supplemental Table S1) and DMT-1 protein levels (Fig. 7A and supplemental Table S2)

FBXL5 Regulates Iron Metabolism in Vivo

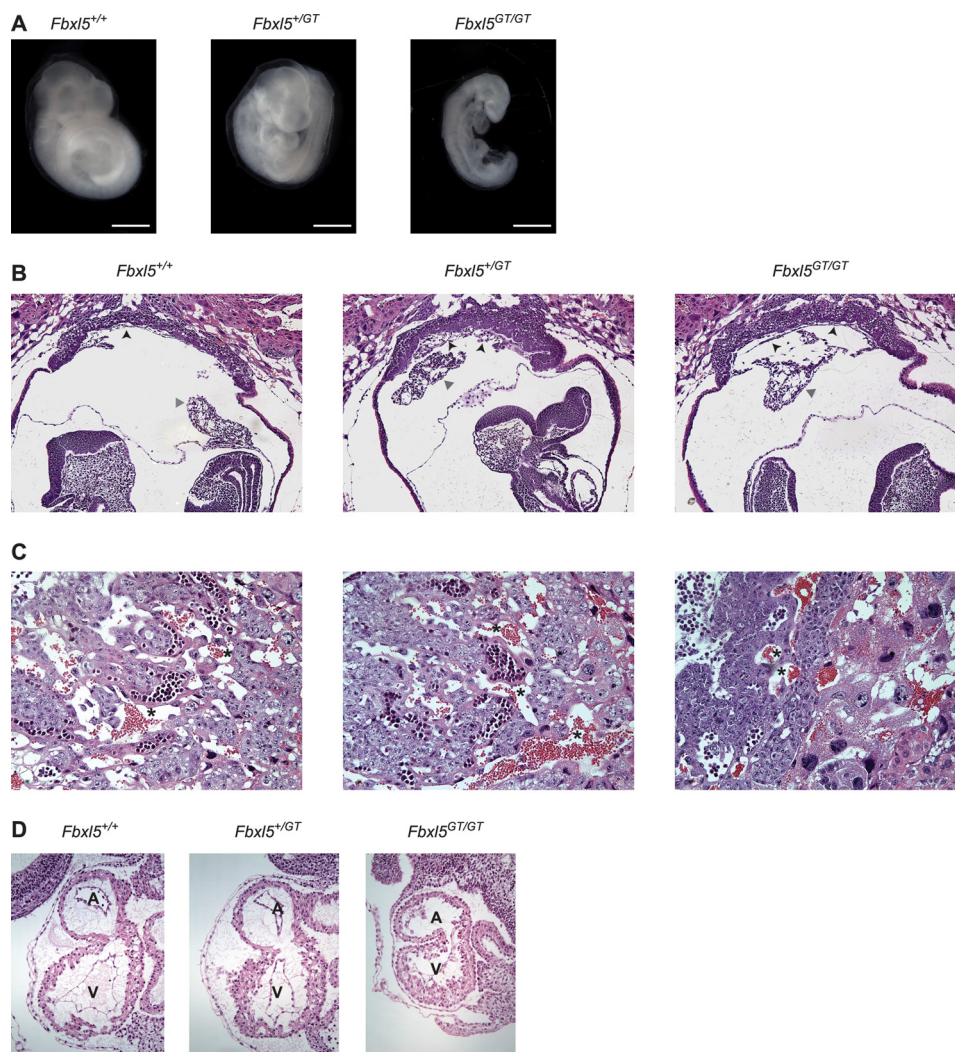


FIGURE 3. Characterization of *Fbxl5*^{GT/GT} embryos. A, *Fbxl5*^{GT/GT} embryos exhibit growth retardation with respect to their wild type (*Fbxl5*^{+/+}) and heterozygous (*Fbxl5*^{+/GT}) littermates. Embryos were harvested at day E9.5 and fixed in 4% paraformaldehyde. Bar, 1 mm. B, *Fbxl5*^{GT/GT} embryos undergo normal placentation. Histological analysis (H&E stained) of sagittal section of *Fbxl5*^{+/+}, *Fbxl5*^{+/GT}, and *Fbxl5*^{GT/GT} embryos (E9.0) reveals formation of the chorioallantoic plate (allantois, gray arrows; chorioallantoic plate, black arrows) and (C) maternal (*) and fetal blood mixing in the chorioallantoic plate. D, *Fbxl5*^{GT/GT} embryos have normal heart development. Histological analysis (H&E stained) of sagittal sections of *Fbxl5*^{+/+}, *Fbxl5*^{+/GT}, and *Fbxl5*^{GT/GT} embryonic hearts (E9.0). A, atrium; V, ventricle.

in the *Fbxl5*^{+/GT} duodenum samples. Interestingly, this enhanced IRP responsiveness appears to be primarily limited to the intestine as the expression of iron metabolism genes was identical between wild type and heterozygous livers (Fig. 7B), spleens, and brains (supplemental Tables S1 and S2). Similar results were observed in syngeneic *Fbxl5*^{+/GT} mice (supplemental Fig. S3). Interestingly, through *Irp2*^{-/-}; *Fbxl5*^{GT/GT} mice are viable, the lack of FBXL5 was not sufficient to reverse the anemia that accompanies *Irp2* deletion.⁴ This result further supports a role for IRP2 in mediating the erythropoietic phenotypes observed in *Fbxl5* heterozygotes.

DISCUSSION

FBXL5 plays a critical role in the maintenance of cellular iron homeostasis (8, 9). Here we show that previous *in vitro* findings extend to a required *in vivo* role for FBXL5. Global inactivation of the *Fbxl5* gene results in embryonic lethality, with growth

defects readily apparent prior to day E9 despite normal placentation, gastrulation, and cardiovascular development. Cells derived from FBXL5-null embryos are unable to sufficiently degrade IRP2 when incubated in the presence of excess iron and are apt to import iron that cannot be appropriately sequestered within the limiting amount of ferritin available. Using an independently generated *Fbxl5* knock-out mouse, it was recently shown that FBXL5-null embryos accumulate excess ferrous iron and are exposed to damaging levels of oxidative stress (15). Although many E3 ligases ubiquitinate multiple substrates (29), simultaneous inactivation of both the *Fbxl5* and *Irp2* genes is sufficient to rescue embryonic lethality, also consistent with the prior report (15).

Despite sharing >70% identity (30), the mechanisms by which the IRE-binding activity of IRP1 and IRP2 are inactivated in iron-replete cells largely differ (31). Both FBXL5-mediated degradation (8, 9) and IRE recognition of IRP1 are inactivated by iron upon insertion of an iron-sulfur cluster (31–33), although the contribution of protein degradation to *in vivo*

⁴ J. C. Ruiz and R. K. Bruick, unpublished results.

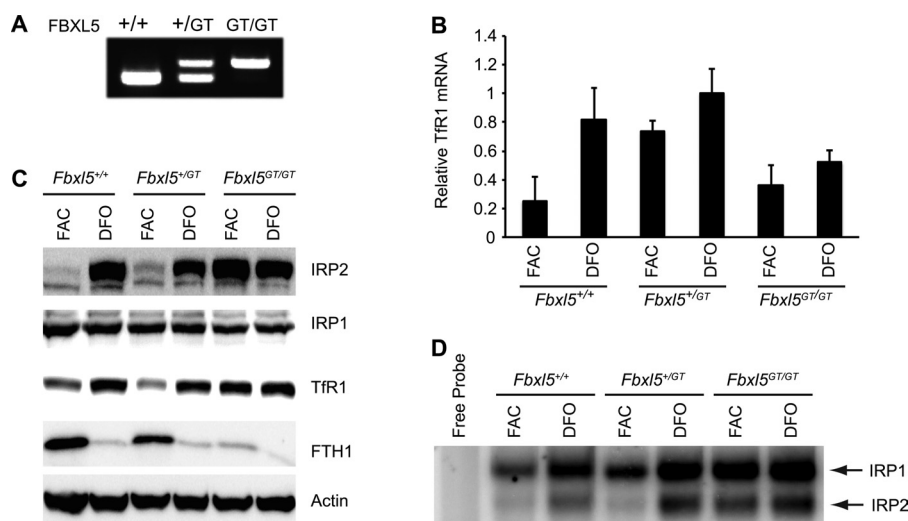


FIGURE 4. Iron metabolism genes are aberrantly regulated in *FBXL5^{GT/GT}* mouse embryonic cells. *A*, mouse embryonic cells genotypes assessed by PCR assay (Fig. 2). *B*, relative TfR1 mRNA accumulation measured by quantitative PCR (supplemental Table S3). Each column represents the average of three experiments \pm S.D. *C*, immunoblot analysis of IRPs and their targets (supplemental Table S4) from mouse embryonic cells treated with FAC and DFO. Actin levels were assessed as a loading control. *D*, assessment of RNA binding activity from mouse embryonic cells treated with ferric ammonium citrate (FAC) or deferoxamine mesylate (DFO).

TABLE 2

Genotypes of mice produced from *Fbx15^{+ /GT}*; *Irp2^{+ /-}* intercrosses

p value for the Chi square test was 0.0698 indicating that the genotype distribution was not significantly different from expected Mendelian ratios.

	No. of animals			Total
	<i>Irp2^{+ /+}</i>	<i>Irp2^{+ /-}</i>	<i>Irp2^{- /-}</i>	
<i>Fbx15^{+ /+}</i>	11	20	7	38
<i>Fbx15^{+ /GT}</i>	24	36	7	67
<i>Fbx15^{GT /GT}</i>	0	0	5	5
Total	35	56	19	110

TABLE 3

Genotypes of mice produced from *Fbx15^{+ /GT}*; *Irp1^{+ /-}* intercrosses

p value for the Chi-Square test was 0.0042 indicating that the genotype distribution was significantly different from expected Mendelian ratios.

	No. of animals			Total
	<i>Irp1^{+ /+}</i>	<i>Irp1^{+ /-}</i>	<i>Irp1^{- /-}</i>	
<i>Fbx15^{+ /+}</i>	37	54	21	112
<i>Fbx15^{+ /GT}</i>	39	124	37	200
<i>Fbx15^{GT /GT}</i>	0	0	0	0
Total	76	178	58	312

TABLE 4

Hematological parameters and serum values from *Fbx15^{+ /+}* and *Fbx15^{+ /GT}* mice fed either an iron sufficient or low iron diet

Values are expressed as mean \pm S.D. of 12 replicates. In the rows, differences between paired values denoted by superscript letters are statistically significant as determined by *t* test.

	<i>Fbx15^{+ /+}</i>		<i>Fbx15^{+ /GT}</i>	
	Sufficient Fe	Low Fe	Sufficient Fe	Low Fe
RBC (M/ μ l)	9.2 \pm 0.3	7.6 \pm 0.4 ^a	9.2 \pm 0.2	9.3 \pm 0.4 ^a
Hematocrit (%)	53 \pm 2	33 \pm 2 ^b	51 \pm 2	49 \pm 2 ^b
Hemoglobin (g/dl)	13.8 \pm 0.3	9.9 \pm 0.8 ^c	13.0 \pm 0.4	13.0 \pm 0.5 ^c
Iron (μ g/dl)	253 \pm 20	58 \pm 10	252 \pm 5	53 \pm 10
TIBC (μ g/dl)	337 \pm 8	504 \pm 9	334 \pm 26	556 \pm 34
Saturation (%)	75 \pm 6	12 \pm 1	78 \pm 5	10 \pm 2

^a *p* = 0.006.
^b *p* < 0.001.
^c *p* < 0.005.

IRP1 regulation is not completely understood (8, 9, 32, 34). In extracts from both mouse embryonic cells and the duodenum, IRE binding by IRP1 is enhanced upon partial or complete *FBXL5* inactivation (Fig. 4D), even though total IRP1 protein

TABLE 5

Hematological parameters and serum values from syngeneic *Fbx15^{+ /+}* and *Fbx15^{+ /GT}* mice fed either an iron sufficient or low iron diet

Values expressed as mean \pm S.D. of 3 replicates. In the rows, differences between paired values denoted by superscript letters are statistically significant as determined by *t* test.

	<i>Fbx15^{+ /+}</i>		<i>Fbx15^{+ /GT}</i>	
	Sufficient Fe	Low Fe	Sufficient Fe	Low Fe
RBC (M/ μ l)	9.9 \pm 0.3	7.0 \pm 0.5 ^a	8.9 \pm 1.1	8.7 \pm 0.2 ^a
Hematocrit (%)	51.4 \pm 1.3	28.5 \pm 1.8 ^b	49 \pm 2	45 \pm 3 ^b
Hemoglobin (g/dl)	15.2 \pm 0.3	9.2 \pm 0.6 ^c	15 \pm 1	12.6 \pm 0.3 ^c
Iron (μ g/dl)	285 \pm 36	57 \pm 13	298 \pm 48	51 \pm 10
TIBC (μ g/dl)	343 \pm 20	576 \pm 18	333 \pm 28	579 \pm 14
Saturation (%)	87 \pm 5	11 \pm 4	89 \pm 11	9.7 \pm 1.7

^a *p* = 0.003.
^b *p* < 0.005.
^c *p* < 0.001.

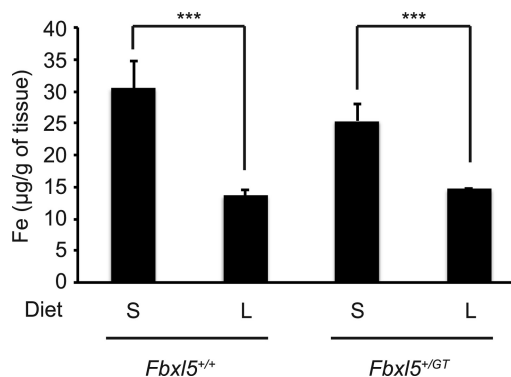


FIGURE 5. Total iron concentration in *Fbx15^{+ /+}* and *Fbx15^{+ /GT}* mice. The iron (Fe) content in perfused livers from *Fbx15^{+ /+}* and *Fbx15^{+ /GT}* mice fed either an iron-sufficient (S; 50 ppm) or a low (L; 5 ppm) iron diet for 3 weeks was determined by inductively coupled plasma mass spectrometry. Each column represents the average of 4 mice \pm S.D. and statistically significant differences were determined by *t* test: ***, *p* < 0.001; **, *p* < 0.003; *, *p* < 0.05.

accumulation remains relatively constant (Fig. 4C). However, if only a small percentage of IRP1 protein were competent for RNA binding, as is the case in liver and perhaps other tissues (23, 32, 35), significant changes in the accumulation of this apo form may be difficult to detect over the background of bulk holo-IRP1. Alternatively, iron-sulfur cluster assembly on IRP1

FBXL5 Regulates Iron Metabolism in Vivo

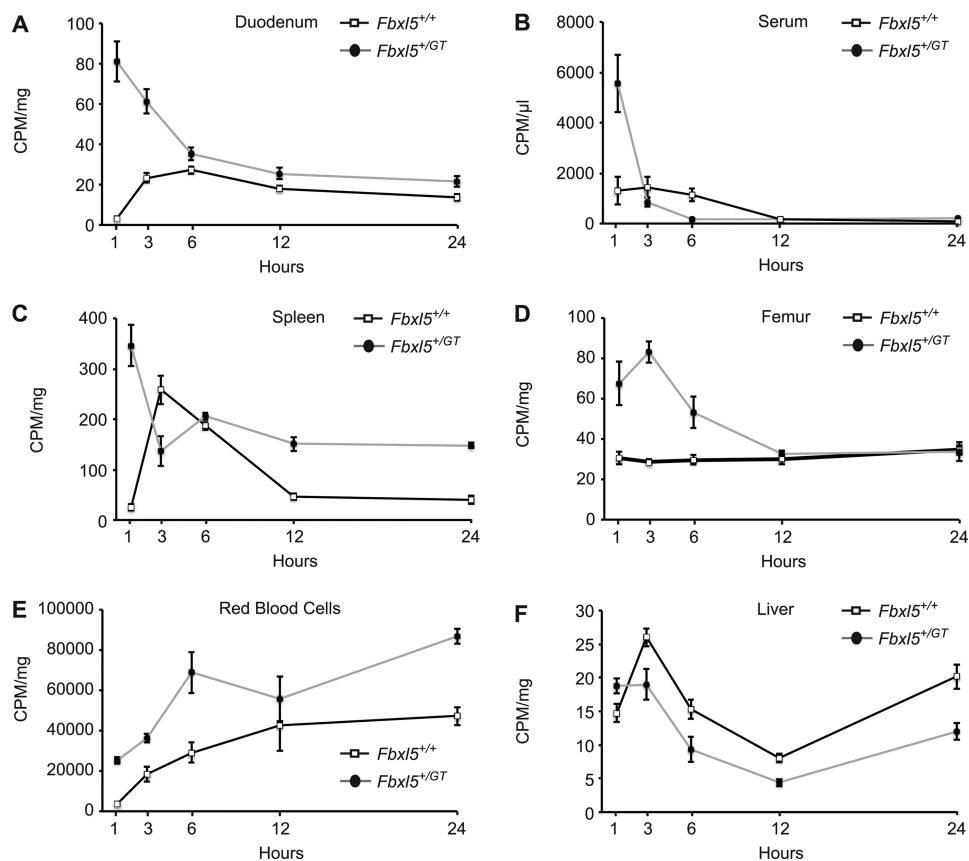


FIGURE 6. ***Fbx15*^{+/*GT*} mice fed a low iron diet for 3 weeks have altered ⁵⁹Fe absorption and distribution profiles compared with wild type littermates.** ⁵⁹Fe levels were measured in the (A) duodenum, (B) serum, (C) spleen, (D) femur, (E) red blood cells, and (F) liver at the indicated time points. Each point represents the average values from 4 mice ± S.D.

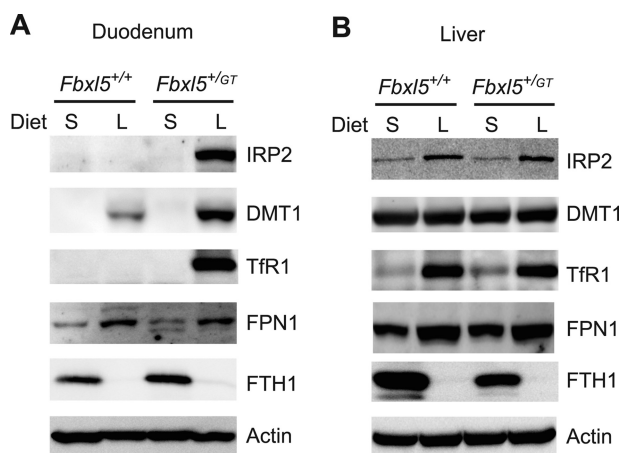


FIGURE 7. **The duodena of *FBXL5*^{+/*GT*} mice display a heightened responsiveness to a low iron diet.** Immunoblot analysis of IRP2 and its targets DMT1, TfR1, ferroportin (*FPN1*), and ferritin heavy chain 1 (*FTH1*) in the duodenum (A) and liver (B) of *FBXL5*^{+/*+*} and *FBXL5*^{+/*GT*} mice fed either an iron-sufficient (S; 50 ppm) or low (L; 5 ppm) iron diet for 3 weeks. Actin levels were assessed as a loading control. Quantitation is provided in supplemental Table S2.

may be compromised in *FBXL5*-deficient cells as a result of increased oxidative stress (31, 36) or some other mechanism.

Nevertheless, although IRP1 and IRP2 are thought to bind many of the same mRNA targets *in vivo* and are thought to be largely redundant (16, 17, 22, 23, 37), simultaneous inactivation of the *IRP1* gene product did not rescue the embryonic lethality in *FBXL5*-null mice (Table 3). If rescue of embryonic lethality

upon IRP2 ablation were solely due to a reduction in total IRE-binding capacity, IRP1 inactivation might have been expected to result in similar compensatory changes given that IRP1 and IRP2 have comparable RNA binding capacities in both the mouse embryonic cells and duodenum. Although indicating that IRP1 and IRP2 have distinct physiological roles, these results cannot distinguish between possible underlying mechanisms including IRP2-selective IRE targets (38), differences in temporal and spatial expression patterns (Fig. 1), or differential IRP responsiveness in the context of stresses such as hypoxia (39).

In addition to the similar results observed upon global *FBXL5* inactivation, Moroishi and colleagues (15) also constructed a mouse model in which *FBXL5* was selectively ablated in the liver. Although viable, these mice exhibited both cell-autonomous effects, including hallmarks of liver damage, and systemic effects, consisting of increased serum iron levels likely due to decreased hepcidin expression in the liver. When challenged with a high iron diet, severe iron overload was restricted to the liver and proved fatal within a day (15). In this context, the distinct phenotype we observed with the heterozygous *Fbx15*^{+/*GT*} mice was of particular interest in at least two key respects: 1) the phenotype was manifested with a low iron diet and 2) the phenotype suggests that the intestine has distinct iron-sensing characteristics that may underlie a more privileged role in the maintenance of systemic iron homeostasis in response to iron deficiency than previously appreciated.

Fbxl5 heterozygosity had no observed effect on the behavior of most tissues we examined, including the liver, either from animals fed a low iron (5 ppm) or iron-sufficient (50 ppm) diet (Fig. 7B and supplemental Table S2). We also saw no difference in animals fed standard chow that contains excess iron (250 ppm, data not shown),⁵ although it remains possible that new phenotypes could emerge in the *Fbxl5*^{+/*GT*} mice when challenged with supraphysiological dietary iron. Nevertheless, *Fbxl5*^{+/*GT*} mice fed a low iron diet were more effective than their wild type littermates at absorbing iron and maintaining hematocrit and hemoglobin levels, despite no differences in the expression levels of traditional systemic regulators of iron mobilization (liver hepcidin) or erythropoiesis (renal erythropoietin) (supplemental Table S1). These systemic adaptations were mirrored by corresponding changes in gene expression within the duodenum, including increased induction of IRP2 protein levels, IRE-binding capacity, and DMT-1 expression (Fig. 7, A and C, and supplemental Table S1). Tfr1 also contains IREs within its 3' UTR (40) and likewise accumulates in the intestines of the *Fbxl5*^{+/*GT*} mice fed the low iron diet (Fig. 7A and supplemental Table S1), although the relevance of this observation is unclear as Tfr1 is not responsible for iron uptake from the lumen. Because IRP2 levels are normal in mice fed an iron-sufficient diet (Fig. 7A), there does not appear to be an overall diminished capacity for IRP degradation. Rather, the intestines of these heterozygotes are responding as though they were further iron-deficient than their wild type counterparts. Despite sharing this same FBXL5 iron-sensor, the iron "set point" of the duodenum appears distinct from most other tissues. Importantly, these characteristics were observed in mice having either isogenic (Table 5 and supplemental Fig. S3) or mixed genetic backgrounds.

Although the serum values in Table 4 reflect steady-state measurements, the flux measurements in Fig. 6 clearly show preferential targeting of serum iron to the erythron. It remains unclear as to whether the liver "refuses" iron or whether the erythron is more effective in its capture. Immature RBC have much higher Tfr1 levels than hepatocytes (41), and it remains possible that iron homeostasis is also altered in erythropoietic tissues to further facilitate uptake of absorbed iron, although we detected no comparable changes in gene expression in the spleen (supplemental Tables S1 and S2).

These results validate an important physiological role for the iron-sensing FBXL5 protein in the regulation of IRPs and maintenance of both cellular and systemic iron homeostasis. Cells lacking FBXL5 expression fail to recognize their metabolic iron status and continuously accumulate toxic levels of bioavailable iron in an unregulated fashion. The damage incurred in iron-replete livers lacking FBXL5 suggests that it may be a genetic modifier of hemochromatosis (15). FBXL5 also plays a role in establishing IRP responsiveness even when iron is limiting, as revealed by the altered behavior of the duodenum in *Fbxl5* heterozygotes. Because these mice maintain normal hematocrit and hemoglobin levels, a partial inhibition of FBXL5 expression may also have physiological benefits, as iron deficiency is the

most common nutritional disorder worldwide (2). Last, as revealed upon FBXL5 depletion, the intestine has iron-responsive characteristics distinct from those of other tissues, conferring the capacity to influence systemic iron homeostasis in a previously unappreciated manner. It will be of great interest to investigate those responsible factors that work in conjunction with the FBXL5 iron sensor to establish the homeostatic iron set point in different cell types.

Acknowledgments—We thank Sean McCormick and Paul A. Lindahl for inductively coupled plasma mass spectrometry analysis, Sandi Jo Estill, James Richardson, and the UTSW Molecular Pathology Core for assistance with the animal studies, C. Nizzi and N. Keuler for statistical analysis, and members of the Bruick lab for helpful advice. This investigation was conducted in a facility constructed with support from the Research Facilities Improvement Program Grant C06 RR 15437-01 from the National Center for Research Resources.

REFERENCES

1. Camaschella, C., and Poggiali, E. (2011) Inherited disorders of iron metabolism. *Curr. Opin. Pediatr.* **23**, 14–20
2. Grosbois, B., Decaux, O., Cador, B., Cazalets, C., and Jego, P. (2005) Human iron deficiency. *Bull. Acad. Natl. Med.* **189**, 1649–1663; discussion 1663–1664
3. Rouault, T. A. (2006) The role of iron regulatory proteins in mammalian iron homeostasis and disease. *Nat. Chem. Biol.* **2**, 406–414
4. Hentze, M. W., Muckenthaler, M. U., Galy, B., and Camaschella, C. (2010) Two to tango. Regulation of mammalian iron metabolism. *Cell* **142**, 24–38
5. Thomson, A. M., Rogers, J. T., and Leedman, P. J. (1999) Iron-regulatory proteins, iron-responsive elements and ferritin mRNA translation. *Int. J. Biochem. Cell Biol.* **31**, 1139–1152
6. Koeller, D. M., Casey, J. L., Hentze, M. W., Gerhardt, E. M., Chan, L. N., Klausner, R. D., and Harford, J. B. (1989) A cytosolic protein binds to structural elements within the iron regulatory region of the transferrin receptor mRNA. *Proc. Natl. Acad. Sci. U.S.A.* **86**, 3574–3578
7. Guo, B., Phillips, J. D., Yu, Y., and Leibold, E. A. (1995) Iron regulates the intracellular degradation of iron regulatory protein 2 by the proteasome. *J. Biol. Chem.* **270**, 21645–21651
8. Salahudeen, A. A., Thompson, J. W., Ruiz, J. C., Ma, H. W., Kinch, L. N., Li, Q., Grishin, N. V., and Bruick, R. K. (2009) An E3 ligase possessing an iron-responsive hemerythrin domain is a regulator of iron homeostasis. *Science* **326**, 722–726
9. Vashist, A. A., Zumbrennen, K. B., Huang, X., Powers, D. N., Durazo, A., Sun, D., Bhaskaran, N., Persson, A., Uhlen, M., Sangfelt, O., Spruck, C., Leibold, E. A., and Wohlschlegel, J. A. (2009) Control of iron homeostasis by an iron-regulated ubiquitin ligase. *Science* **326**, 718–721
10. Shu, C., Sung, M. W., Stewart, M. D., Igumenova, T. I., Tan, X., and Li, P. (2012) The structural basis of iron sensing by the human F-box protein FBXL5. *Chembiochem.* **13**, 788–791
11. Thompson, J. W., Salahudeen, A. A., Chollangi, S., Ruiz, J. C., Brautigam, C. A., Makris, T. M., Lipscomb, J. D., Tomchick, D. R., and Bruick, R. K. (2012) Structural and molecular characterization of iron-sensing hemerythrin-like domain within F-box and leucine-rich repeat protein 5 (FBXL5). *J. Biol. Chem.* **287**, 7357–7365
12. Chollangi, S., Thompson, J. W., Ruiz, J. C., Gardner, K. H., and Bruick, R. K. (2012) Hemerythrin-like domain within F-box and leucine-rich repeat protein 5 (FBXL5) communicates cellular iron and oxygen availability by distinct mechanisms. *J. Biol. Chem.* **287**, 23710–23717
13. Thompson, J. W., and Bruick, R. K. (2012) Protein degradation and iron homeostasis. *Biochim. Biophys. Acta.* **1823**, 1484–1490
14. Salahudeen, A. A., and Bruick, R. K. (2009) Maintaining mammalian iron and oxygen homeostasis. Sensors, regulation, and cross-talk. *Ann. N.Y. Acad. Sci.* **1177**, 30–38

⁵ J. C. Ruiz and R. K. Bruick, unpublished data.

FBXL5 Regulates Iron Metabolism in Vivo

- Moroishi, T., Nishiyama, M., Takeda, Y., Iwai, K., and Nakayama, K. I. (2011) The FBXL5-IRP2 axis is integral to control of iron metabolism *in vivo*. *Cell Metab.* **14**, 339–351
- Galy, B., Ferring, D., and Hentze, M. W. (2005) Generation of conditional alleles of the murine iron regulatory protein (IRP)-1 and -2 genes. *Genesis* **43**, 181–188
- Galy, B., Ferring, D., Minana, B., Bell, O., Janser, H. G., Muckenthaler, M., Schümann, K., and Hentze, M. W. (2005) Altered body iron distribution and microcytosis in mice deficient in iron regulatory protein 2 (IRP2). *Blood* **106**, 2580–2589
- Lee, J., Petris, M. J., and Thiele, D. J. (2002) Characterization of mouse embryonic cells deficient in the Ctr1 high affinity copper transporter. Identification of a Ctr1-independent copper transport system. *J. Biol. Chem.* **277**, 40253–40259
- Popescu, B. F., Robinson, C. A., Rajput, A., Rajput, A. H., Harder, S. L., and Nichol, H. (2009) Iron, copper, and zinc distribution of the cerebellum. *Cerebellum*. **8**, 74–79
- Guo, B., Brown, F. M., Phillips, J. D., Yu, Y., and Leibold, E. A. (1995) Characterization and expression of iron regulatory protein 2 (IRP2). Presence of multiple IRP2 transcripts regulated by intracellular iron levels. *J. Biol. Chem.* **270**, 16529–16535
- Galy, B., Ferring, D., Benesova, M., Benes, V., and Hentze, M. W. (2004) Targeted mutagenesis of the murine IRP1 and IRP2 genes reveals context-dependent RNA processing differences *in vivo*. *RNA* **10**, 1019–1025
- LaVaute, T., Smith, S., Cooperman, S., Iwai, K., Land, W., Meyron-Holtz, E., Drake, S. K., Miller, G., Abu-Asab, M., Tsokos, M., Switzer, R., 3rd, Grinberg, A., Love, P., Tresser, N., and Rouault, T. A. (2001) Targeted deletion of the gene encoding iron regulatory protein-2 causes misregulation of iron metabolism and neurodegenerative disease in mice. *Nat. Genet.* **27**, 209–214
- Meyron-Holtz, E. G., Ghosh, M. C., Iwai, K., LaVaute, T., Brazzolotto, X., Berger, U. V., Land, W., Ollivierre-Wilson, H., Grinberg, A., Love, P., and Rouault, T. A. (2004) Genetic ablations of iron regulatory proteins 1 and 2 reveal why iron regulatory protein 2 dominates iron homeostasis. *EMBO J.* **23**, 386–395
- Ross, K. L., and Eisenstein, R. S. (2002) Iron deficiency decreases mitochondrial aconitase abundance and citrate concentration without affecting tricarboxylic acid cycle capacity in rat liver. *J. Nutr.* **132**, 643–651
- Galy, B., Ferring-Appel, D., Kaden, S., Gröne, H. J., and Hentze, M. W. (2008) Iron regulatory proteins are essential for intestinal function and control key iron absorption molecules in the duodenum. *Cell Metab.* **7**, 79–85
- Mastrogiannaki, M., Matak, P., Keith, B., Simon, M. C., Vaulont, S., and Peyssonnaud, C. (2009) HIF-2 α , but not HIF-1 α , promotes iron absorption in mice. *J. Clin. Invest.* **119**, 1159–1166
- Ganz, T., and Nemeth, E. (2012) Hepcidin and iron homeostasis. *Biochim. Biophys. Acta.* **1823**, 1434–1443
- De Domenico, I., Ward, D. M., and Kaplan, J. (2011) Hepcidin and ferroportin. The new players in iron metabolism. *Semin. Liver Dis.* **31**, 272–279
- Ho, M. S., Ou, C., Chan, Y. R., Chien, C. T., and Pi, H. (2008) The utility F-box for protein destruction. *Cell Mol. Life Sci.* **65**, 1977–2000
- Pantopoulos, K. (2004) Iron metabolism and the IRE/IRP regulatory system. An update. *Ann. N.Y. Acad. Sci.* **1012**, 1–13
- Eisenstein, R. S. (2000) Iron regulatory proteins and the molecular control of mammalian iron metabolism. *Annu. Rev. Nutr.* **20**, 627–662
- Clarke, S. L., Vasanthakumar, A., Anderson, S. A., Pondarré, C., Koh, C. M., Deck, K. M., Pitula, J. S., Epstein, C. J., Fleming, M. D., and Eisenstein, R. S. (2006) Iron-responsive degradation of iron-regulatory protein 1 does not require the Fe-S cluster. *EMBO J.* **25**, 544–553
- Pantopoulos, K., Gray, N. K., and Hentze, M. W. (1995) Differential regulation of two related RNA-binding proteins, iron regulatory protein (IRP), and IRPB. *RNA* **1**, 155–163
- Wang, J., Fillebeen, C., Chen, G., Biederbick, A., Lill, R., and Pantopoulos, K. (2007) Iron-dependent degradation of apo-IRP1 by the ubiquitin-proteasome pathway. *Mol. Cell. Biol.* **27**, 2423–2430
- Chen, O. S., Schalinke, K. L., and Eisenstein, R. S. (1997) Dietary iron intake modulates the activity of iron regulatory proteins and the abundance of ferritin and mitochondrial aconitase in rat liver. *J. Nutr.* **127**, 238–248
- Mueller, S., Pantopoulos, K., Hübner, C. A., Stremmel, W., and Hentze, M. W. (2001) IRP1 activation by extracellular oxidative stress in the perfused rat liver. *J. Biol. Chem.* **276**, 23192–23196
- Smith, S. R., Ghosh, M. C., Ollivierre-Wilson, H., Hang Tong, W., and Rouault, T. A. (2006) Complete loss of iron regulatory proteins 1 and 2 prevents viability of murine zygotes beyond the blastocyst stage of embryonic development. *Blood Cells Mol. Dis.* **36**, 283–287
- Butt, J., Kim, H. Y., Basilion, J. P., Cohen, S., Iwai, K., Philpott, C. C., Altschul, S., Klausner, R. D., and Rouault, T. A. (1996) Differences in the RNA binding sites of iron regulatory proteins and potential target diversity. *Proc. Natl. Acad. Sci. U.S.A.* **93**, 4345–4439
- Schneider, B. D., and Leibold, E. A. (2003) Effects of iron regulatory protein regulation on iron homeostasis during hypoxia. *Blood* **102**, 3404–3411
- Leibold, E. A., and Guo, B. (1992) Iron-dependent regulation of ferritin and transferrin receptor expression by the iron-responsive element binding protein. *Annu. Rev. Nutr.* **12**, 345–368
- Ponka, P., and Lok, C. N. (1999) The transferrin receptor: role in health and disease. *Int. J. Biochem. Cell Biol.* **31**, 1111–1137